Electronic Supplementary Information (ESI)

Molecular recognition of planar and non-planar aromatic hydrocarbons through multipoint Ag–π bonding in a dinuclear metallo-macrocycle

Kenichiro Omoto, Shohei Tashiro and Mitsuhiko Shionoya*

Department of Chemistry, Graduate School of Science, The University of Tokyo
7-3-1 Hongo, Bunkyo-ku, Tokyo 113-0033, Japan

1. Abbreviation

COSY: correlated spectroscopy, Et_2O: diethyl ether, ESI-TOF: electrospray ionization-time-of-flight, THF: tetrahydrofurane, NMR: nuclear magnetic resonance, TMS: tetramethylsilane, XRD: X-ray diffraction, PXRD: powder X-ray diffraction, DSC: differential scanning calorimetry,

2. Materials and methods

All solvents, organic and inorganic reagents are commercially available, and were used without further purification. Macrocyclic ligand **L1**, dinuclear Ag^I-complex $[Ag_2\mathbf{L1}X_2](SbF_6)_2$ (X = Et_2O or H_2O) were prepared according to previously reported procedures.[1]

NMR spectroscopic measurements were performed using a Bruker AVANCE 500 (500 MHz for ^1H) spectrometer. NMR spectra were calibrated as below; tetramethylsilane ($Si(CH_3)_4$) = 0 ppm for ^1H in $CDCl_3$. *p*-Dimethoxybenzene was added as an internal standard for the calibration of the concentration of samples. ESI-TOF mass spectra were recorded on a Micromass LCT spectrometer and a Micromass LCT Premier spectrometer. Single-crystal X-ray crystallographic analyses were performed using a Rigaku RAXIS-RAPID imaging plate diffractometer with Mo$K\alpha$ radiation, and the obtained data were calculated using a CrystalStructure crystallographic software package except for refinement, which was performed using SHELXL-97.[2] Molecular modeling was performed by a Spartan'08 based on MMFF97 as a force field.

3. Guest binding behaviors of $[Ag_2L1X_2](SbF_6)_2$

Complexation of $[Ag_2L1X_2](SbF_6)_2$ and anthracene

^{1}H NMR titration experiment at 300 K

To a solution of $[Ag_2\mathbf{L1}X_2](SbF_6)$ in $CDCl_3$ (0.11 mM, 475 μL, 0.052 μmol, 1.0 eq) was added a solution of anthracene (**Ant**) in $CDCl_3$ (20 mM). Curve fitting of the obtained data determined a stability constant K_a(**Ant**) = [**Ant**⊂$[Ag_2\mathbf{L1}]^{2+}$]/([**Ant**][$[Ag_2\mathbf{L1}X_2]^{2+}$]) to be $(3.0 \pm 0.4) \times 10^4\ M^{-1}$ in $CDCl_3$ at 300 K.

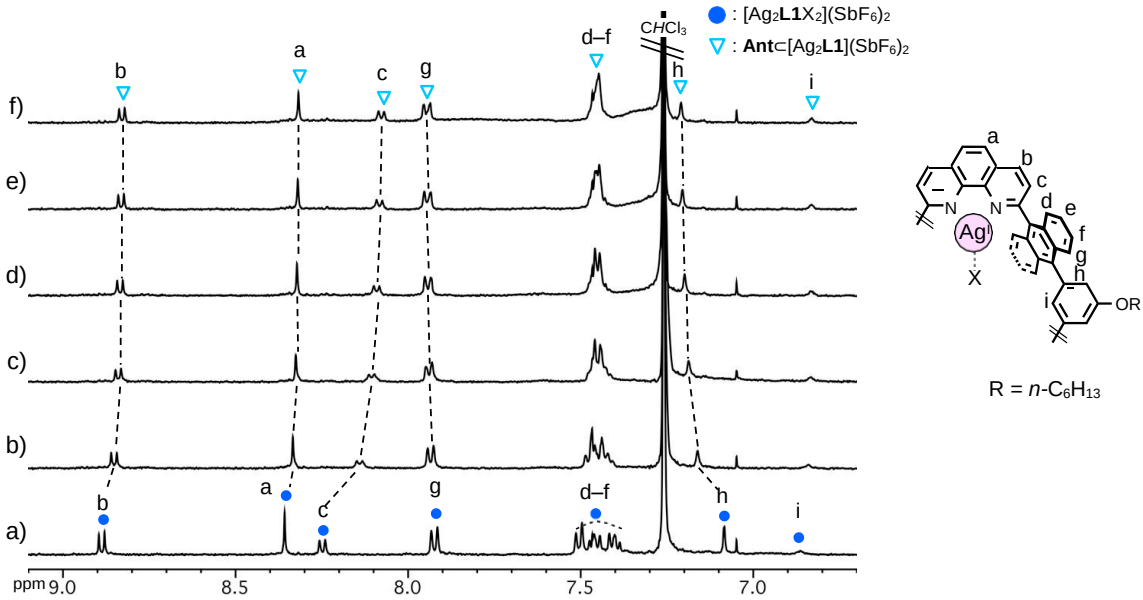

Fig. S1. Partial ^{1}H NMR spectra of $[Ag_2\mathbf{L1}X_2](SbF_6)_2$ (0.11 mM) in the presence of a) 0.0, b) 1.0, c) 2.0, d) 3.0, e) 4.0, and f) 5.0 eq of **Ant** (500 MHz, $CDCl_3$, 300 K).

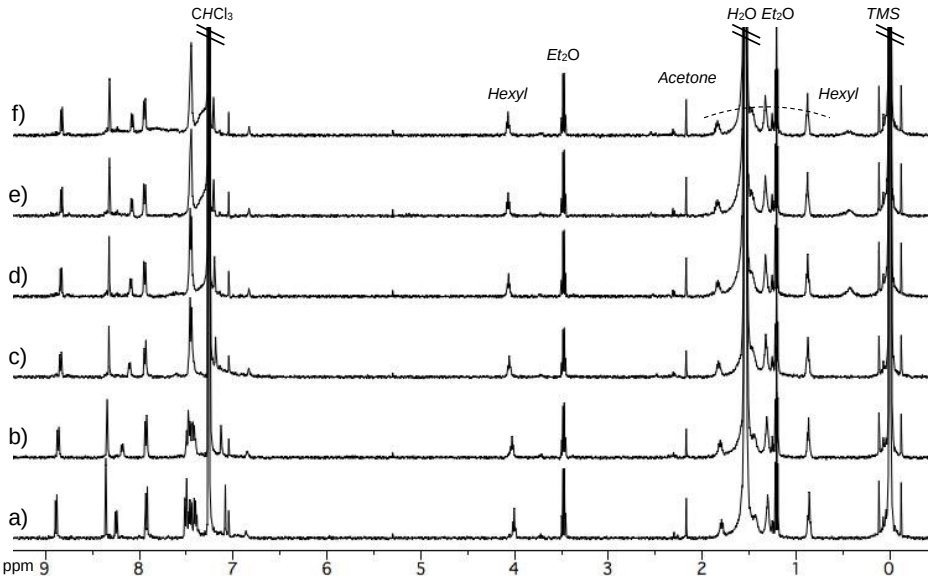

Fig. S2. ^{1}H NMR spectra of $[Ag_2\mathbf{L1}X_2](SbF_6)_2$ (0.11 mM) in the presence of a) 0.0, b) 1.0, c) 2.0, d) 3.0, e) 4.0, and f) 5.0 eq of **Ant** (500 MHz, $CDCl_3$, 300 K).

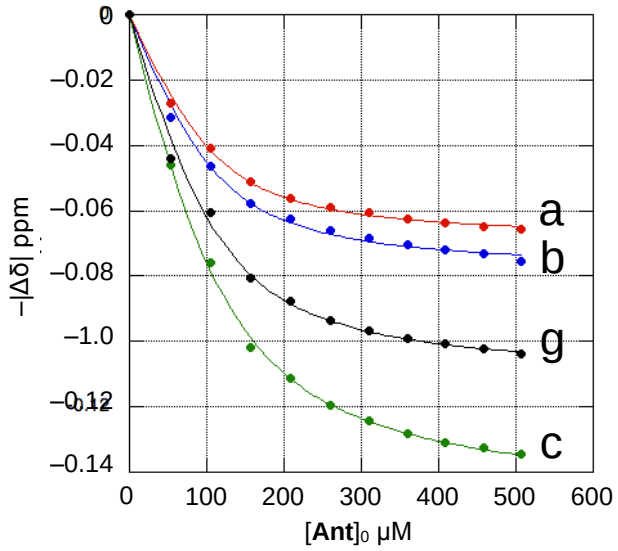

$$K_a(\mathbf{Ant}) = \frac{[\mathbf{Ant}\subset[Ag_2\mathbf{L1}]^{2+}]}{[\mathbf{Ant}]\,[[Ag_2\mathbf{L1}X_2]^{2+}]}$$

$$= (3.0 \pm 0.4) \times 10^4\ M^{-1}$$

in $CDCl_3$ at 300 K

Fig. S3. Stability constant analysis by the least square fitting to the shift of NMR signals ($H_{a–c, g}$) in the titration experiment described in Figs. S1–S2 (solid circles: observed, lines: calculated). [**Ant**]$_0$indicates the initial concentration of **Ant**.

^{1}H NMR titration experiment at 220 K

To a solution of $[Ag_2\mathbf{L1}X_2](SbF_6)_2$ in $CDCl_3$ (0.07 mM, 450 μL, 0.029 μmol, 1.0 eq) was added a solution of anthracene (**Ant**) in $CDCl_3$ (20 mM).

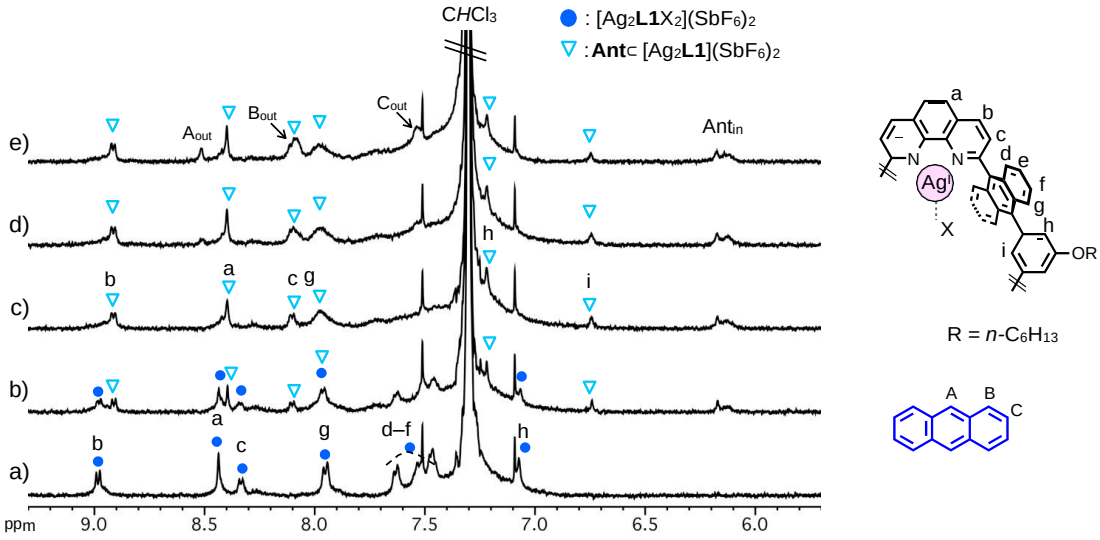

Fig. S4. Partial ^{1}H NMR spectra of $[Ag_2\mathbf{L1}X_2](SbF_6)_2$ (0.07 mM) in the presence of a) 0.0, b) 0.5, c) 1.0, d) 1.5, and e) 2.0 eq of **Ant** (500 MHz, $CDCl_3$, 220 K). $\mathbf{Ant_{in}}$ represents the signals of included **Ant**.

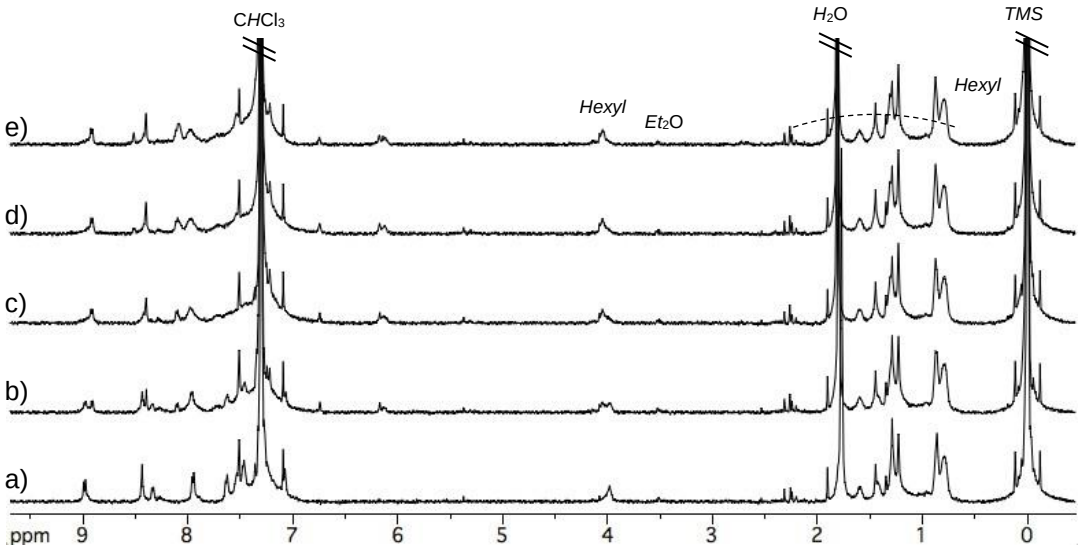

Fig. S5. ^{1}H NMR spectra of $[Ag_2\mathbf{L1}X_2](SbF_6)_2$ (0.07 mM) in the presence of a) 0.0, b) 0.5, c) 1.0, d) 1.5, and e) 2.0 eq of **Ant** (500 MHz, $CDCl_3$, 220 K).

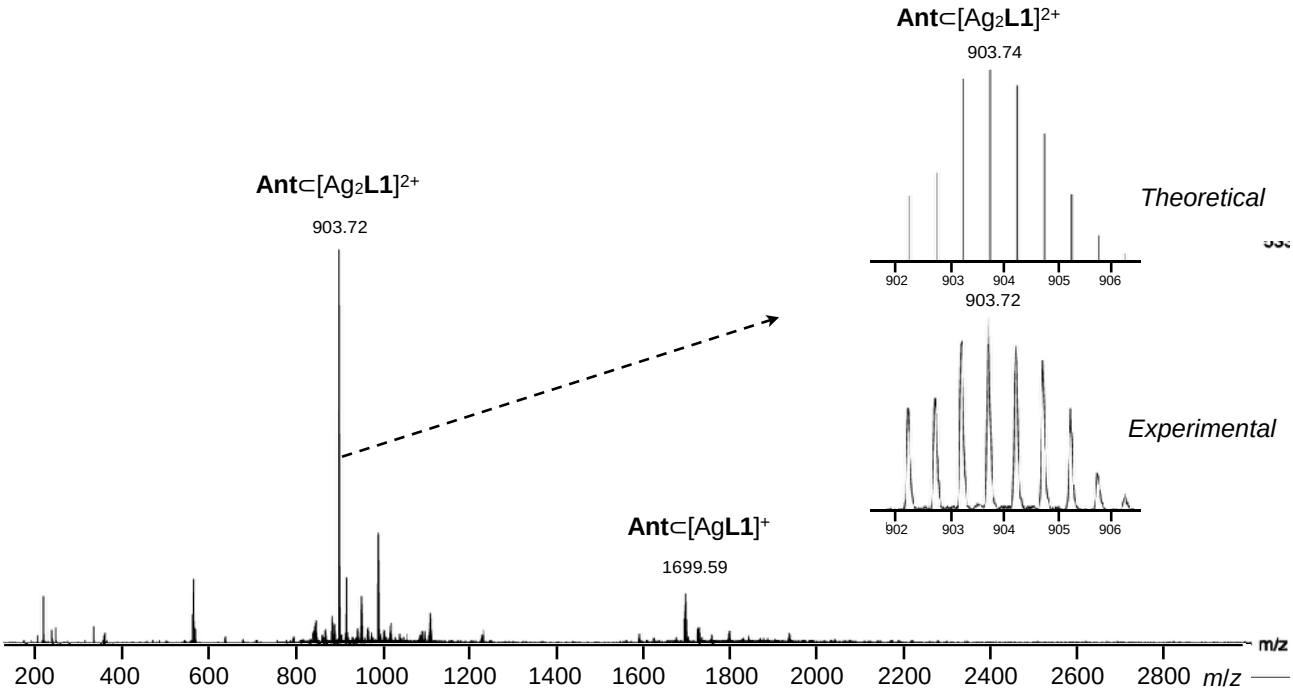

Fig. S6. ESI-TOF mass spectrum of a mixture of $[Ag_2\mathbf{L1}X_2](SbF_6)_2$ and 5.0 eq of **Ant** in $CHCl_3$.

Crystallization of Ant⊂[Ag_2L1(CH_2Cl_2)$_2$](SbF_6)$_2$·(C_5H_{12})$_2$·(CH_2Cl_2)$_2$

To a suspension of **L1** (0.23 mM, 450 μL, 0.10 μmol, 1.0 eq) in $CHCl_3$ was added a solution of $AgSbF_6$ (200 mM, 2.1 μL, 0.42 μmol, 4.2 eq) in acetone and a solution of **Ant** (200 mM, 5.2 μL, 1.0 μmol, 10 eq) in $CHCl_3$ to obtain a clear yellow solution. The solvent was once removed by evaporation under reduced pressure. Then a resulting solid was dissolved in CH_2Cl_2 (250 μL). Yellow brock crystals suitable for single crystals XRD measurement were obtained after *n*-pentane vapor diffusion in the dark over about 10 days.

Crystal data of Ant⊂[Ag_2L1(CH_2Cl_2)$_2$](SbF_6)$_2$·(C_5H_{12})$_2$·(CH_2Cl_2)$_2$

Crystal data of $C_{132}H_{118}Ag_2Cl_8F_{12}N_4O_2Sb_2$: F_w = 2763.25, crystal dimensions 0.30 × 0.30 × 0.10 mm^3, monoclinic, space group $P2_1/c$, a = 18.8596(8), b = 13.4589(6), c = 23.972(1) Å, β = 99.096(1)°, V = 6008.3(5) Å^3, Z = 2, ρ_{calcd} = 1.527 g cm^{-3}, μ = 1.0146 mm^{-1}, T = 93 K, λ(MoKα) = 0.71075 Å, 2θ_{max} = 50.0°, 46007/10551 reflection collected/unique (R_{int} = 0.0485), R_1 = 0.0773 ($I > 2\sigma(I)$), wR_2 = 0.2257 (for all data), GOF = 1.025, largest diff. peak and hole 2.84/–1.48 eÅ^{-3}. CCDC deposit number 1911739.

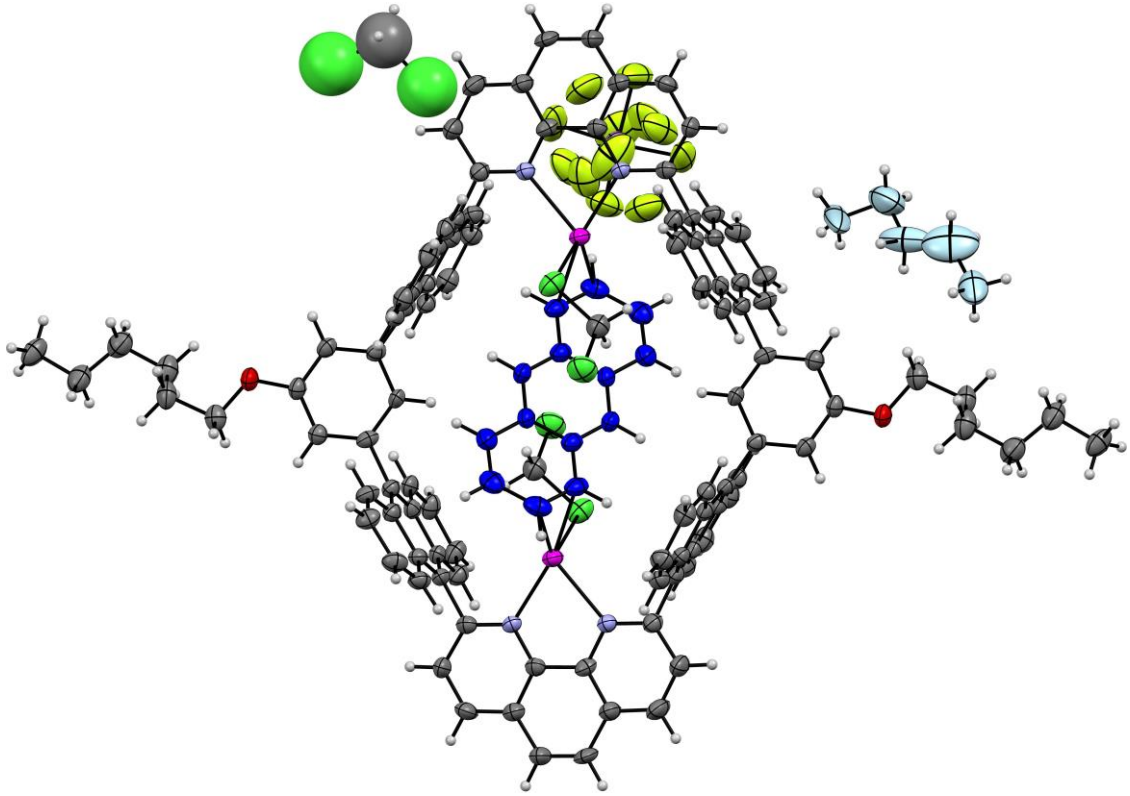

Fig. S7. ORTEP view (50% probability level) of **Ant**⊂[Ag_2**L1**(CH_2Cl_2)$_2$](SbF_6)$_2$·(C_5H_{12})$_2$·(CH_2Cl_2)$_2$. (Ag: magenta, C: grey, C of **Ant**: blue, C of *n*-pentane: pale blue, Cl: pale green, F: yellow, H: white, N: blue, O: red, Sb: purple)

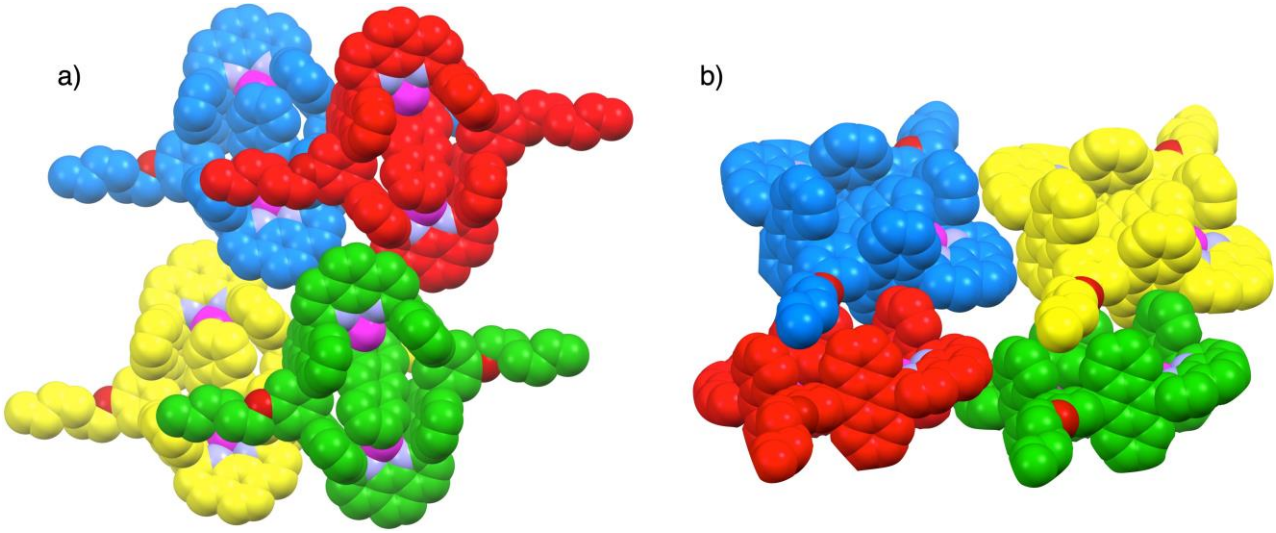

Fig. S8. Crystal packing of **Ant**⊂[Ag_2**L1**(CH_2Cl_2)$_2$](SbF_6)$_2$·(C_5H_{12})$_2$·(CH_2Cl_2)$_2$. (hydrogen atoms, solvents, and counter anions are omitted for clarity). Views from a) *b* axis and b) *c* axis.

Complexation of $[Ag_2L1X_2](SbF_6)_2$ and triptycene

^{1}H NMR titration experiment at 300 K

To a solution of $[Ag_2\mathbf{L1}X_2](SbF_6)_2$ in $CDCl_3$ (0.07 mM, 400 μL, 0.03 μmol, 1.0 eq) was added a solution of triptycene (**Trip**) in $CDCl_3$ (40 mM). Curve fitting of the obtained data determined a stability constant K_a(**Trip**) = [**Trip**⊂$[Ag_2\mathbf{L1}]^{2+}$]/([**Trip**][$[Ag_2\mathbf{L1}X_2]^{2+}$]) to be $(3.1 \pm 0.2) \times 10^4\ M^{-1}$ in $CDCl_3$ at 300 K.

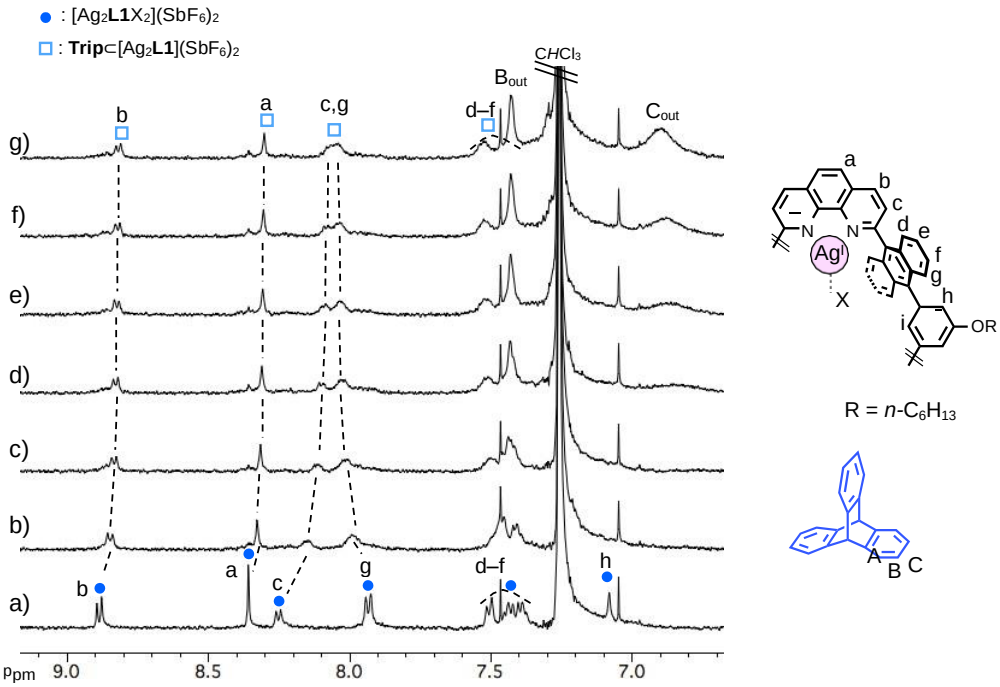

Fig. S9. Partial ^{1}H NMR spectra of $[Ag_2\mathbf{L1}X_2](SbF_6)_2$ (0.07 mM) in the presence of a) 0.0, b) 1.0, c) 2.0, d) 3.0, e) 4.0, f) 5.0, and g) 7.0 eq of **Trip** (500 MHz, $CDCl_3$, 300 K).

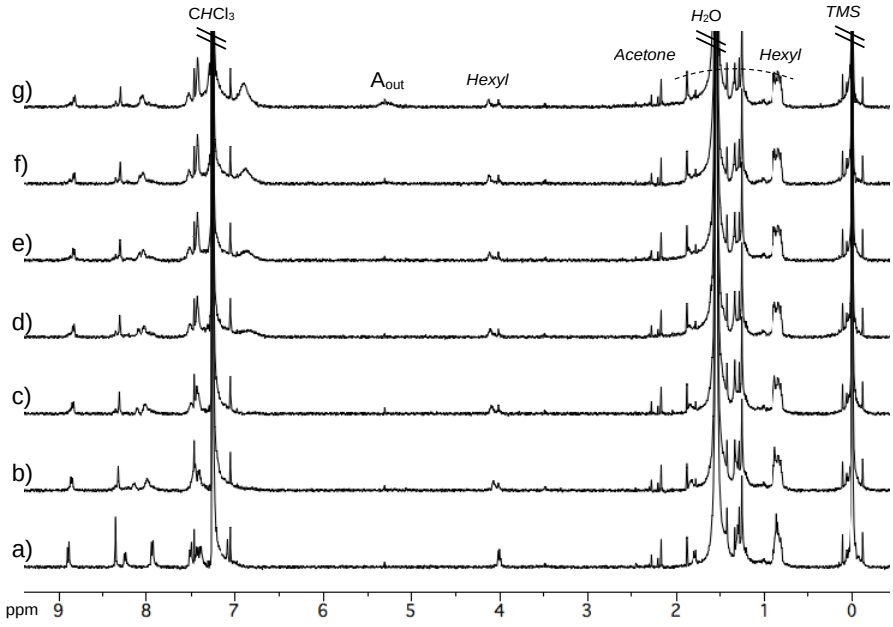

Fig. S10. ^{1}H NMR spectra of $[Ag_2\mathbf{L1}X_2](SbF_6)_2$ (0.07 mM) in the presence of a) 0.0, b) 1.0, c) 2.0, d) 3.0, e) 4.0, f) 5.0, and g) 7.0 eq of **Trip** (500 MHz, $CDCl_3$, 300 K).

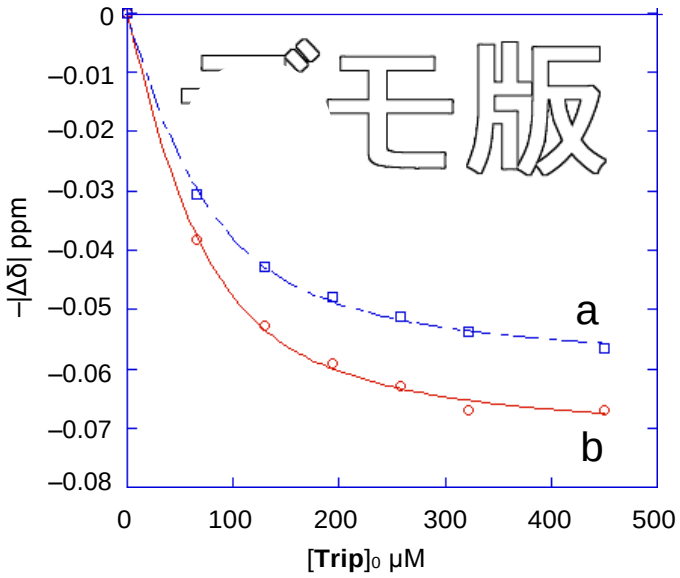

$$K_a(\mathbf{Trip}) = \frac{[\mathbf{Trip}\subset[Ag_2\mathbf{L1}]^{2+}]}{[\mathbf{Trip}]\,[[Ag_2\mathbf{L1}X_2]^{2+}]}$$

$$= (3.1 \pm 0.2) \times 10^4\ M^{-1}$$

in $CDCl_3$ at 300 K

Fig. S11. Stability constant analysis by the least square fitting to the shift of NMR signals ($H_{a,b}$) in the titration experiment described in Figs. S9–S10 (solid circles: observed, lines: calculated). $[\mathbf{Trip}]_0$ indicates the initial concentration of **Trip**.

^{1}H NMR titration experiment at 220 K

To a solution of $[Ag_2\mathbf{L1}X_2](SbF_6)_2$ in $CDCl_3$ (0.11 mM, 450 μL, 0.05 μmol, 1.0 eq) was added a solution of triptycene (**Trip**) in $CDCl_3$ (40 mM).

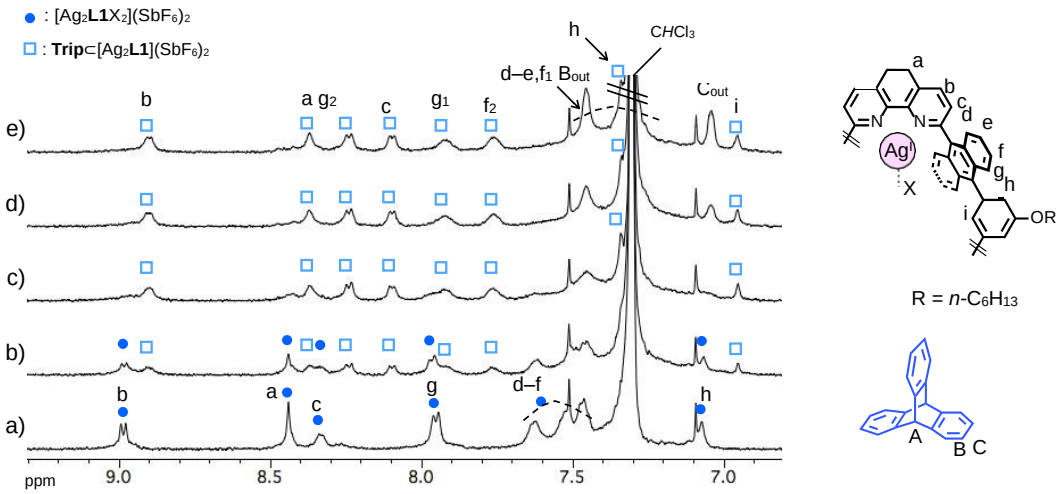

Fig. S12. Partial ^{1}H NMR spectra of $[Ag_2\mathbf{L1}X_2](SbF_6)_2$ (0.11 mM) in the presence of a) 0.0, b) 0.5, c) 1.0, d) 1.5, and e) 2.0 eq of **Trip** (500 MHz, $CDCl_3$, 220 K).

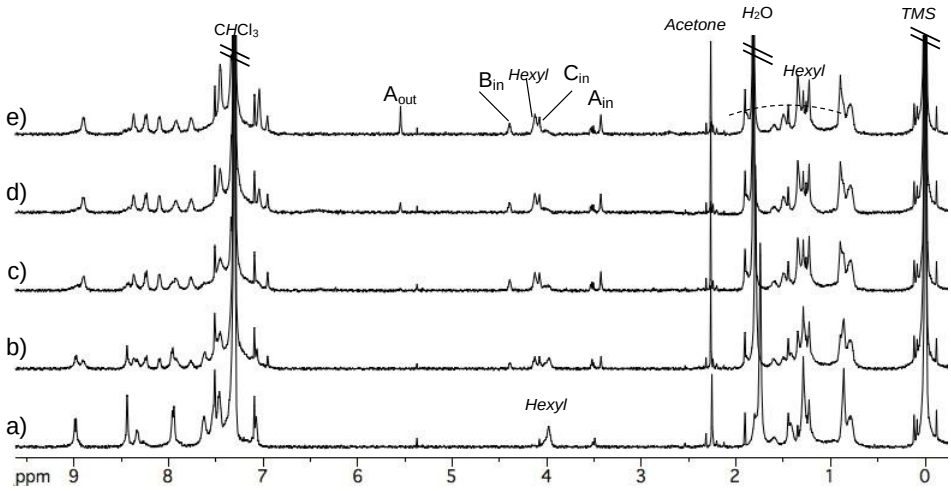

Fig. S13. ^{1}H NMR spectra of $[Ag_2\mathbf{L1}X_2](SbF_6)_2$ (0.11 mM) in the presence of a) 0.0, b) 0.5, c) 1.0, d) 1.5, and e) 2.0 eq of **Trip** (500 MHz, $CDCl_3$, 220 K).

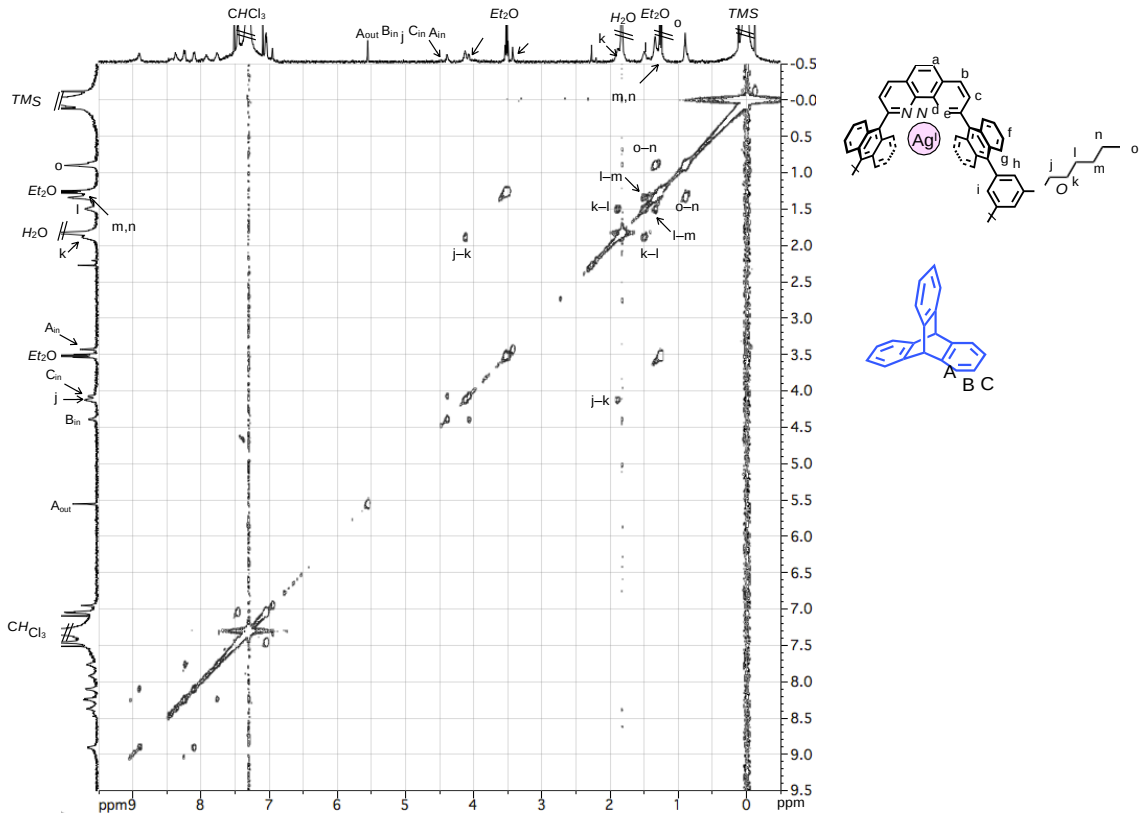

Fig. S14. Partial ^{1}H–^{1}H COSY spectrum of a mixture of $[Ag_2\mathbf{L1}X_2](SbF_6)_2$ (0.07 mM) and **Trip** (2.0 eq) (500 MHz, $CDCl_3$, 220 K).

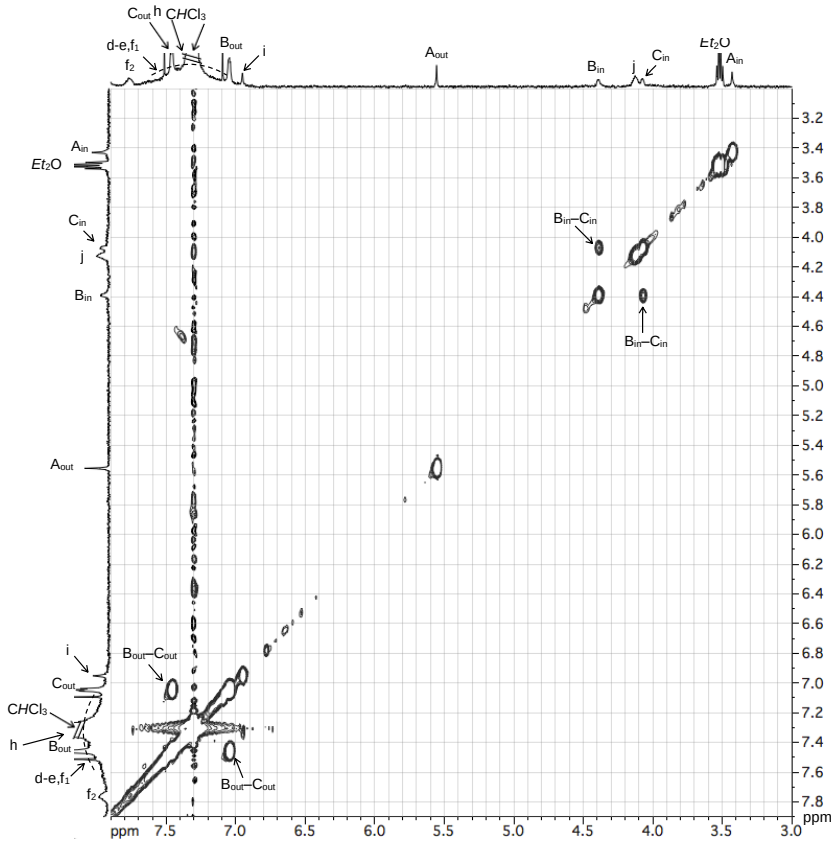

Fig. S15. Partial ^{1}H–^{1}H COSY spectrum of a mixture of $[Ag_2\mathbf{L1}X_2](SbF_6)_2$ (0.07 mM) and **Trip** (2.0 eq) (500 MHz, $CDCl_3$, 220 K).

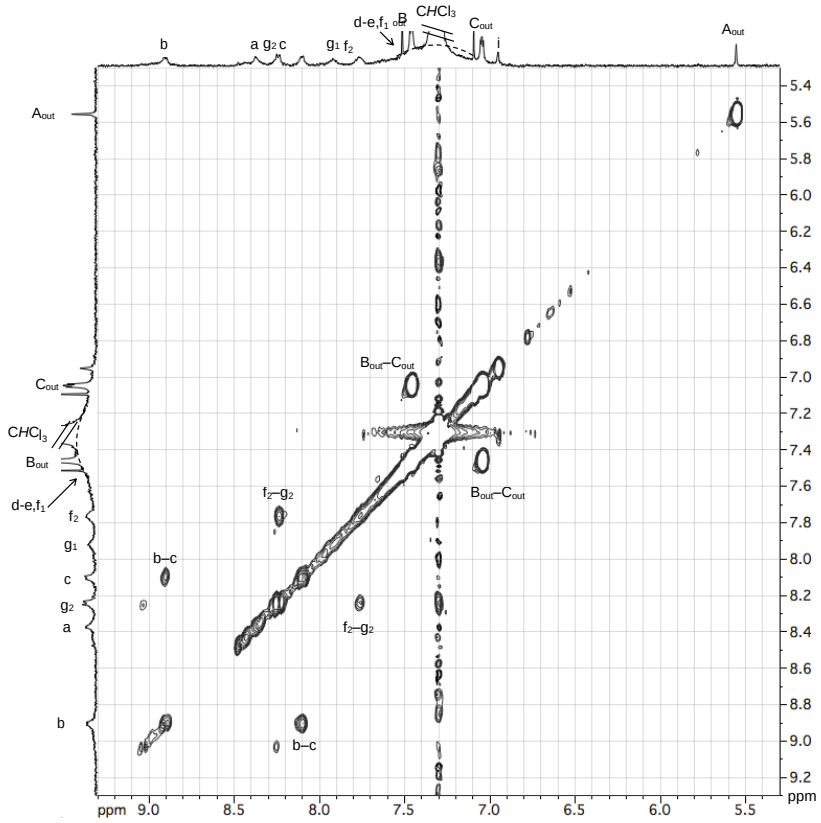

Fig. S16. ^{1}H–^{1}H COSY spectrum of a mixture of $[Ag_2\mathbf{L1}X_2](SbF_6)_2$ (0.07 mM) and **Trip** (2.0 eq) (500 MHz, $CDCl_3$, 220 K).

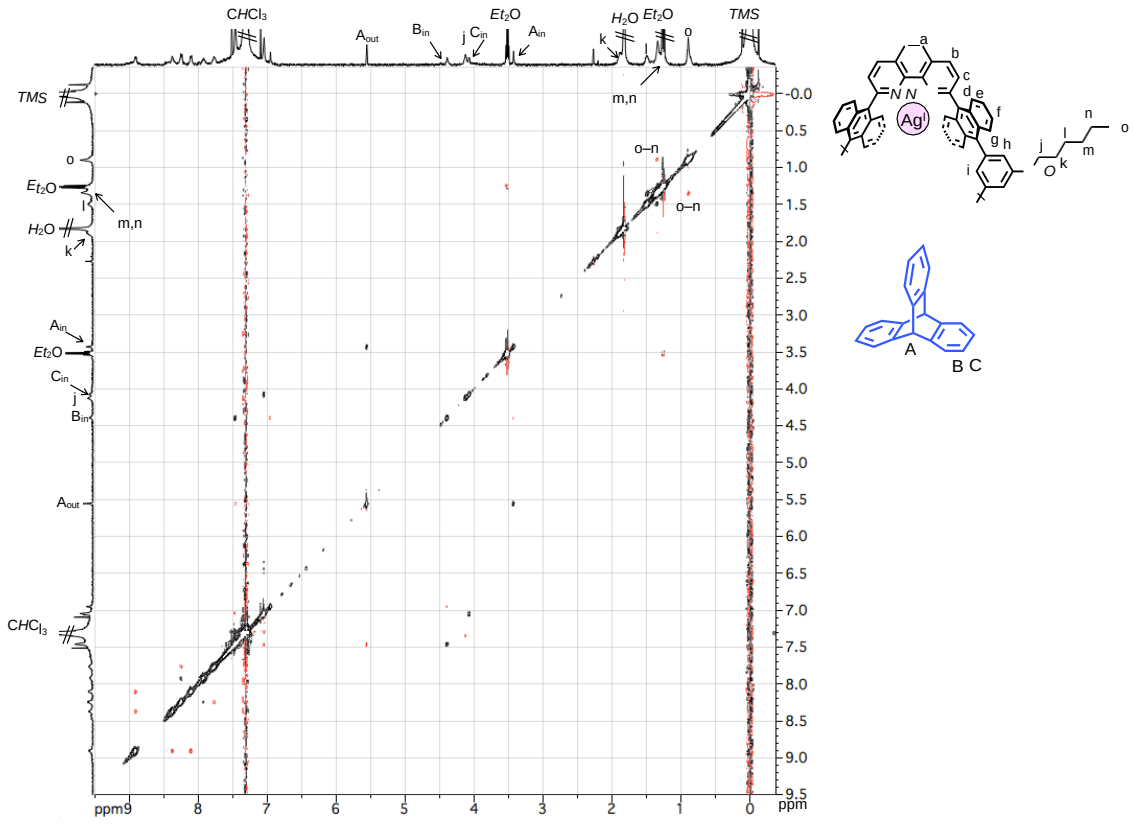

Fig. S17. Partial $^{1}H–^{1}H$ ROESY spectrum of a mixture of $[Ag_2\mathbf{L1}X_2](SbF_6)_2$ (0.07 mM) and **Trip** (2.0 eq) (500 MHz, $CDCl_3$, 220 K).

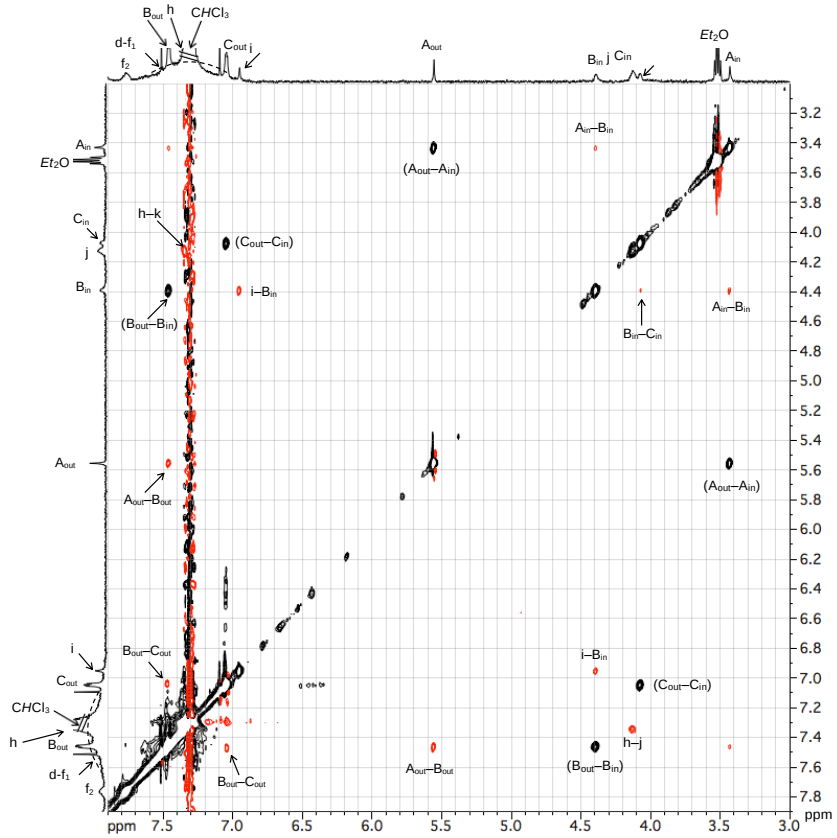

Fig. S18. Partial $^{1}H–^{1}H$ ROESY spectrum of a mixture of $[Ag_2\mathbf{L1}X_2](SbF_6)_2$ (0.07 mM) and **Trip** (2.0 eq) (500 MHz, $CDCl_3$, 220 K). Peaks assigned in parentheses originate from chemical exchange between free and included **Trip**.

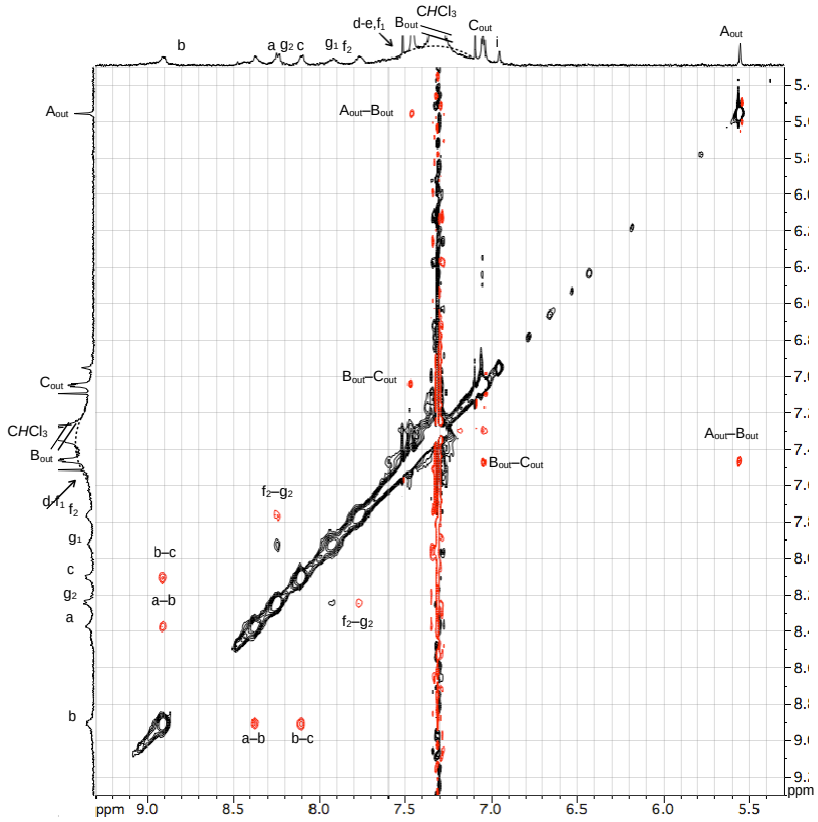

Fig. S19. Partial ^{1}H–^{1}H ROESY spectrum of a mixture of $[Ag_2\mathbf{L1}X_2](SbF_6)_2$ (0.07 mM) and **Trip** (2.0 eq) (500 MHz, $CDCl_3$, 220 K).

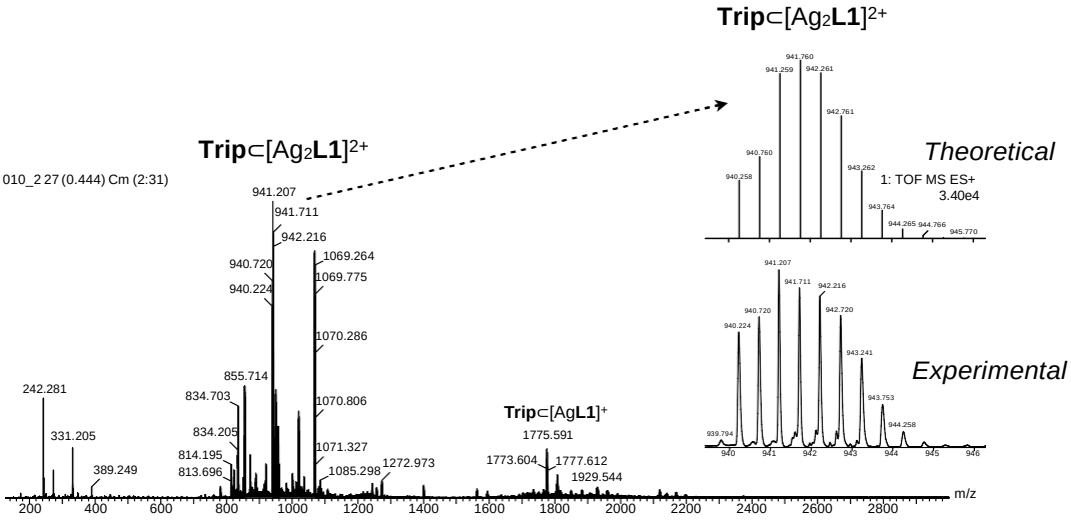

Fig. S20. ESI-TOF mass spectrum of a mixture of $[Ag_2\mathbf{L1}X_2](SbF_6)_2$ and 7.0 eq of **Trip**.

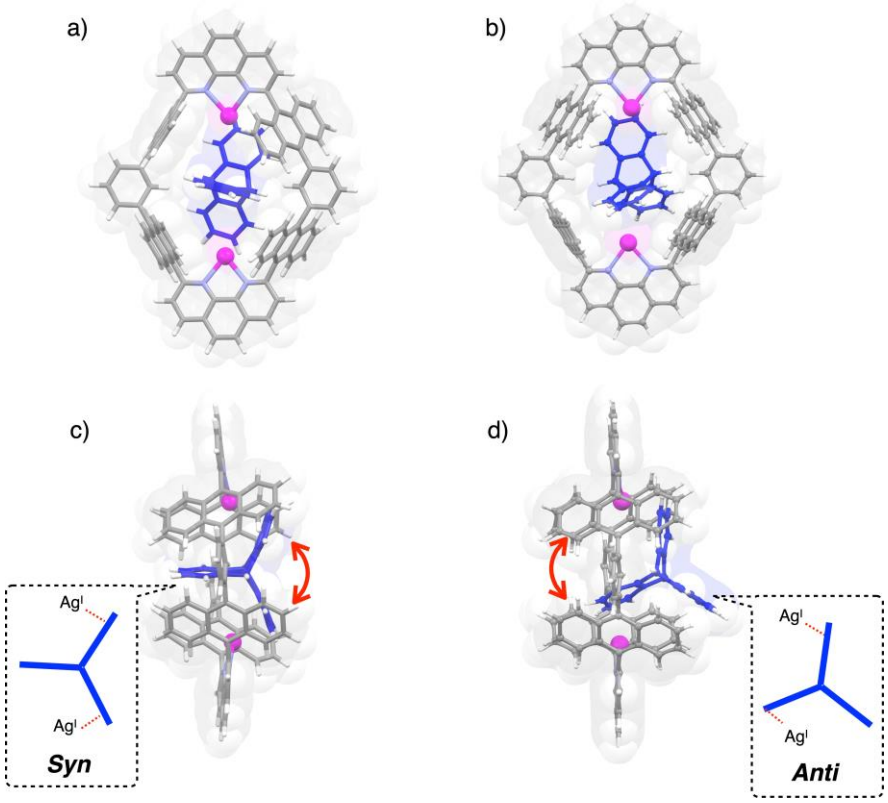

Fig. S21. Possible structures of **Trip**⊂ $[Ag_2\mathbf{L1}]^{2+}$ based on molecular mechanics calculation; a) a front view and c) a side view of a *syn*-isomer; b) a front view and d) a side view of an *anti*-isomer. (Ag: magenta, C: grey, C of **Trip**: blue, H: white, N: blue). Side alkyloxy chains of **L1** are omitted for clarity. Red arrows in Fig. S21c–d represent a possible rotational movement of **Trip** within the nano-space of $[Ag_2\mathbf{L1}]^{2+}$, which causes conservation of 3-fold rotational symmetry of **Trip** in the ^{1}H NMR time scale (Fig. S13).

Complexation of $[Ag_2L1X_2](SbF_6)_2$ and naphthalene

^{1}H NMR titration experiment

To a solution of $[Ag_2\mathbf{L1}X_2](SbF_6)_2$ in $CDCl_3$ (0.11 mM, 475 μL, 0.052 μmol, 1.0 eq) was added a solution of naphthalene in $CDCl_3$ (20 mM).

Complexation of $[Ag_2L1X_2](SbF_6)_2$ and *p*-xylene

^{1}H NMR titration experiment

To a solution of $[Ag_2\mathbf{L1}X_2](SbF_6)_2$ in $CDCl_3$ (0.11 mM, 475 μL, 0.052 μmol, 1.0 eq) was added a solution of *p*-xylene in $CDCl_3$ (9.7 mM).

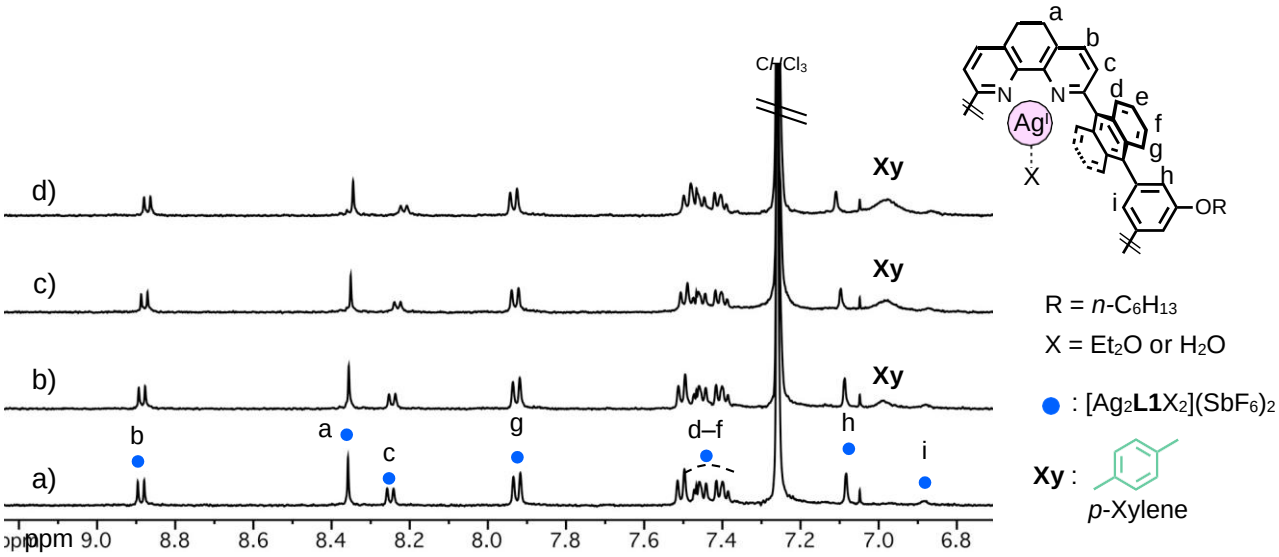

Fig. S22. Partial ^{1}H NMR spectra of $[Ag_2\mathbf{L1}X_2](SbF_6)_2$ (0.11 mM) in the presence of a) 0.0, b) 1.0, c) 3.0, and d) 5.0 eq of *p*-xylene (500 MHz, $CDCl_3$, 300 K).

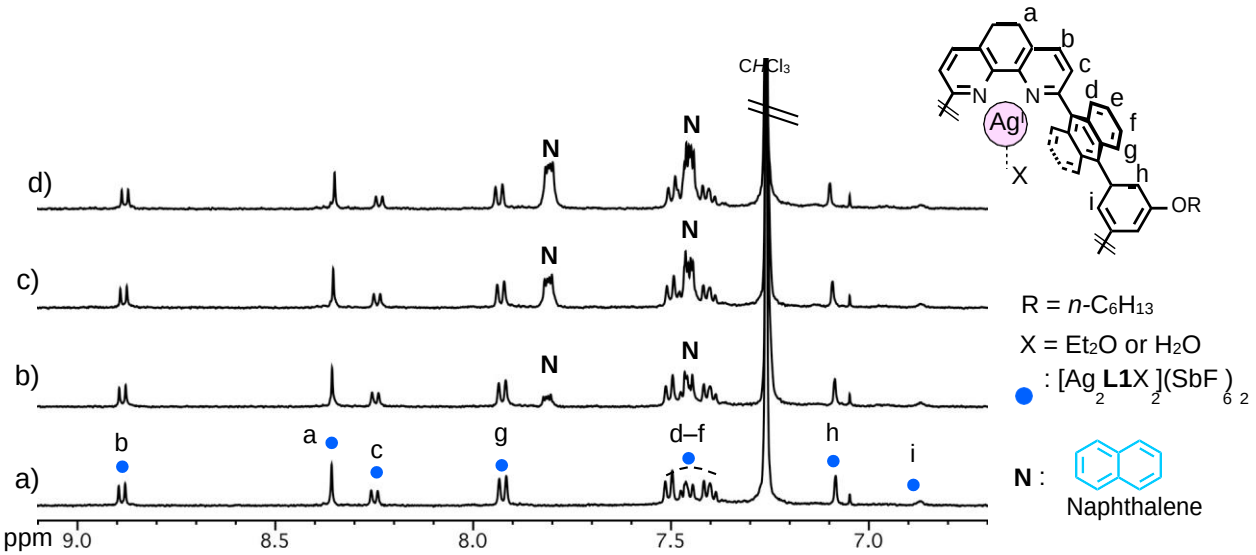

Fig. S23. Partial ^{1}H NMR spectra of $[Ag_2\mathbf{L1}X_2](SbF_6)_2$ (0.11 mM) in the presence of a) 0.0, b) 1.0, c) 3.0, and d) 5.0 eq of naphthalene (500 MHz, $CDCl_3$, 300 K).

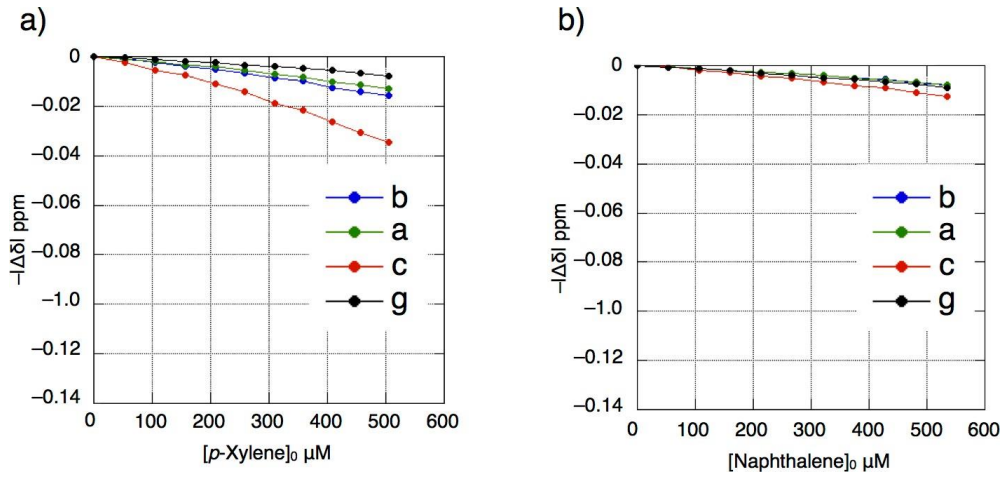

Fig. S24. Plots of the amounts of shift change of the ^{1}H NMR signals ($H_{a–c,g}$) against the concentrations of a) *p*-xylene and b) naphthalene. The spectra are shown in Figs. S22–S23. $[p\text{-Xylene}]_0$ and $[\text{Naphthalene}]_0$ indicate the initial concentrations of *p*-xylene and naphthalene, respectively.

Upon addition of *p*-xylene or naphthalene to a solution of $[Ag_2\mathbf{L1}X_2](SbF_6)_2$ (0.11 mM) in $CDCl_3$, ^{1}H NMR signals of $[Ag_2\mathbf{L1}X_2](SbF_6)_2$ at the aromatic region slightly shifted, but did not converge even in the presence of more than 5.0 eq of guests (Figs. S22–S23). Such almost stationary ^{1}H NMR spectra during titration experiments suggest negligible host-guest interactions or a different binding mode from the 1:1 host-guest structure of **Ant**⊂$[Ag_2\mathbf{L1}]^{2+}$ or **Trip**⊂$[Ag_2\mathbf{L1}]^{2+}$. It should be noted that in the case of titration experiment using **Ant** or **Trip** as guests, the shift of the signals almost converged under the same condition (Figs. S1–S2 and S9–S10).

4. References

1. K. Omoto. S. Tashiro, M. Kuritani and M. Shionoya, *J. Am. Chem. Soc.* 2014, **136**, 17946–17949.
2. G. M. Sheldrick, *SHELXL-97, Program for refinement of crystal structures*, University of Göttingen, Germany, 1997.